ELSEVIER

Journal of Power Sources 90 (2000) 52–58

JOURNAL OF POWER SOURCES

www.elsevier.com/locate/jpowsour

Advanced in situ methods for the characterization of practical electrodes in lithium-ion batteries

P. Novák *, J.-C. Panitz, F. Joho, M. Lanz, R. Imhof [1], M. Coluccia

Laboratory for Electrochemistry, Paul Scherrer Institute, CH-5232 Villigen PSI, Switzerland

Received 14 November 1999; accepted 25 January 2000

Abstract

In this paper, an overview of the progress recently achieved in our laboratory in the development and application of four in situ methods, namely in situ X-ray diffraction measurements (XRD), differential electrochemical mass spectrometry (DEMS), infrared spectroscopy, and Raman microscopy, is presented. For bulk investigations during cycling, in situ XRD measurements are used, and explained here in the instance of the reaction of graphite with lithium. Next, three surface-sensitive in situ methods are discussed, namely DEMS, infrared spectroscopy, and Raman microscopy. As an illustration of in situ infrared spectroscopy and DEMS, we show results for both the oxidative and reductive decomposition of electrolyte solutions. Finally, a cell for in situ Raman microscopy is described. This method is well suited, e.g., for an analysis of the structural properties of carbon materials, for a characterization of positive electrodes, and electrolytes of lithium-ion cells. As an example, Raman spectra measured in situ at a single $LiCoO_2$ particle selected on the surface of a commercial electrode are discussed.

Keywords: Lithium-ion cell; Graphite electrode; Lithium cobalt oxide electrode; Electrolyte decomposition; In situ mass spectrometry; In situ infrared spectroscopy; In situ Raman mapping; In situ X-ray diffraction

1. Introduction

The electrodes used up to now in commercial lithium-ion cells are based on carbon and lithium metal oxides, typically $LiCoO_2$ [1]. Their electrode potentials are far beyond the thermodynamic stability window of organic electrolytes typically used. Hence, apart from chemical and mechanical changes in the electrodes during cycling, electrolyte reduction and oxidation will occur at the interfaces between the electrolyte and the negative and positive electrode, respectively. A better understanding of the mutual interactions of all components in lithium-ion cells is therefore not merely essential for further development; it is one of the current challenges in solid-state electrochemistry. The difficult part is that of extracting the relevant information from working electrodes in situ, because the properties of all possible surface films and also those of the bulk material change to some extent, at least when the electrodes are exposed to moisture, oxygen, and/or CO_2 [2–5]. Moreover, the inevitable exposure of a surface film to vacuum, which occurs when using analytical methods such as X-ray photoelectron spectroscopy or Auger electron spectroscopy, results in a loss of volatile components, shrinkage of the film, and possibly even chemical changes in the surface film.

Hence, the use of in situ analytical tools is advantageous. Conceivable in situ methods are either bulk or surface sensitive. For bulk investigations, in situ X-ray diffraction (XRD) that has been available for more than 20 years [6,7] is the first choice. (Techniques requiring large machines such as a synchrotron, a neutron source, etc., will not be considered here.) Besides, several sophisticated in situ methods suitable for the direct investigation of processes taking place at the electrode/electrolyte interface in organic solutions have been successfully introduced during the last decade, namely differential electrochemical mass spectrometry (DEMS) [8], infrared spectroscopy [9–11], Raman spectroscopy [12,13], scanning tunneling microscopy [14], and ellipsometry [15]. In the following text, an overview of the progress recently achieved in our

* Corresponding author. Tel.: +41-56-310-2457; fax: +41-56-310-4415.

E-mail address: petr.novak@psi.ch (P. Novák).

[1] Present address: Renata AG, CH-4452 Itingen, Switzerland.

0378-7753/00/$ - see front matter
PII: S0378-7753(00)00447-X

laboratory in the development and application of four in situ methods, namely XRD, DEMS, infrared spectroscopy, and Raman microscopy, will be presented. For each method, the corresponding electrochemical cell will be briefly described and, so as to demonstrate the power of any given technique, representative results will be reported.

2. In situ XRD

In lithium-ion batteries, both the negative and positive electrode are made from electronically conductive porous, electrolyte-impregnated composites containing electrochemically active matrix materials able to accommodate (insert, intercalate) variable quantities of lithium ions. As a rule, the lithium insertion/de-insertion into/from the electroactive material results in lattice changes of the insertion host. These changes may be relatively minor (e.g., a small expansion or contraction of the lattice), but can also become major, involving a change in symmetry of the host lattice [16,17]. Both types of insertion-induced changes can be conveniently studied in situ by means of XRD. However, great care must be exercised in designing the cell. This is because XRD probes the bulk of the particles while their potential is determined by the lithium concentration at the particle surfaces. Thus, rapid equilibration of the entire insertion electrode should be achieved in a well-designed cell. Consequently, the current density distribution over the surface of the working electrode should be uniform, while the internal resistance of the cell should be minimized. Moreover, a substantial volume of electrolyte solution is necessary to rapidly supply/store lithium ions consumed/liberated at the working electrode during charging and discharging cycles.

In Fig. 1, we show the schematic drawing of an in situ X-ray cell developed by us, where electrodes from commercial batteries can be used as test samples. The cell, made mainly from stainless steel, is closed off by a thin copper or aluminum foil used, both as a window for the X-ray beam and as a current collector. The foil is irradiated from outside (Fig. 1). The inside of the metal foil is coated with the electrode mass (carbon or lithium metal oxide, binder and, for the positive electrode, carbon as a conductivity enhancer). Many industrial or laboratory processes, such as spray coating or the doctor blade technique, can be used to coat the current collector with the electrode mass. The only restriction is that any potential preferential orientation of the particles should be minimized. Another problem is related to the high intensities of lines corresponding to copper or aluminum, as the metal current collector absorbs part of the rays reflected from the electrode mass, thus reducing significantly the fraction of rays received by the detector. However, this problem can be solved by making the current collector as thin as possible, typically 10–25 μm (this is, in fact, a foil thickness found in commercial electrodes [18]). Even though the scattering from the cell materials (foil and sample holder) is quite prominent and the intensities of the relevant lines reaching the detector are quite low, the line positions are not affected and can be analyzed. As an example, we show lithium intercalation into a special graphite for lithium-ion batteries, Timrex® SLM 44, from a typical industrial electrolyte, 1 M $LiPF_6$ in a 1:1 (w/w) mixture of ethylene carbonate (EC) and dimethyl carbonate (DMC) (battery electrolyte Merck LP30 Selectipur®). The reflections 002 (Fig. 2) and 004 of graphite were readily identified and their shift during lithium intercalation analyzed. The observed line shift is caused by the intercalation of naked lithium ions (without their solvation shells) into the graphite. In such a case, the interlayer distance between the graphene layers increases to a moderate extent (ca. 10% for LiC_6) [19,20].

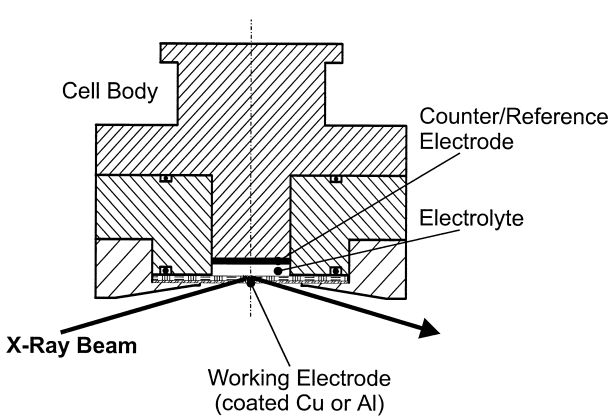

Fig. 1. The electrochemical cell for in situ XRD measurements.

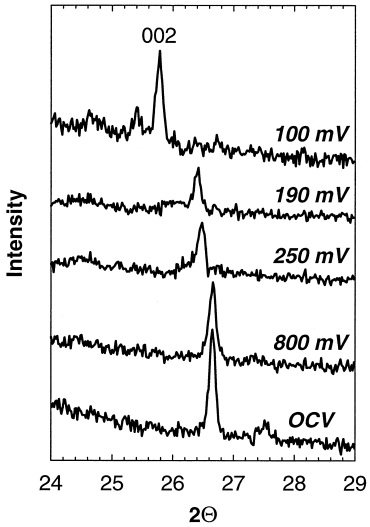

Fig.2. XRD pattern of graphite Timrex® SLM 44 on a 25-μm copper foil, recorded in the in situ X-ray cell using the electrolyte 1 M $LiPF_6$ in EC/DMC (1:1). Potential in mV vs. Li/Li^+; OCV = open-circuit voltage; the traces were shifted vertically.

3. DEMS

One of the most important prerequisites for good cycling stability of lithium-ion batteries is the formation during the initial charge/discharge cycles of a complete and stable passivation film on the negative electrode called the solid electrolyte interphase (SEI) [16,21]. During SEI formation, some gases are evolved, mainly due to reductive decomposition of EC [22]. On the other hand, all the lithium metal oxides commonly used in positive electrodes of Li-ion batteries become highly oxidizing when fully charged (delithiated), and oxidative decomposition of the electrolyte solution resulting in extensive gas evolution can be initiated during cell overcharge [23]. Both effects, electrolyte reduction and oxidation, have been discussed in numerous publications. Unfortunately, most of these studies were performed at model metal electrodes, and care must be exercised when applying such experimental results to real battery electrodes, as their surfaces may exhibit different electrocatalytic activities. Thus, understanding the oxidation and reduction processes occurring in commercial lithium-ion cells at the electrode/electrolyte interfaces remains a major challenge. We have demonstrated that DEMS can yield useful information on these processes, especially when combined with complementary methods such as in situ infrared spectroscopy [23–26].

The DEMS method is based on the non-wettability of a porous membrane that acts as a solvent barrier between the electrochemical cell and the vacuum system of the mass spectrometer. A schematic drawing of our DEMS cell is shown in Fig. 3. A porous working electrode is deposited onto the membrane using a spray coating process such as that described in detail in Ref. [24]. The membrane is the critical component of the cell because it must minimize the evaporation of low-boiling electrolyte components while retaining sufficient permeability for volatile reaction products. These products are pumped off continuously through the membrane during the electrochemical reaction, and are analyzed on-line with a quadrupole mass spectrometer. Hence, intensity changes in mass signals (mass-spectrum cyclic voltammograms, MSCV) can be detected as a function of time and/or potential and, thus, can be correlated with current peaks in the cyclic voltammogram (CV) or plateaus on galvanostatic charging/discharging curves.

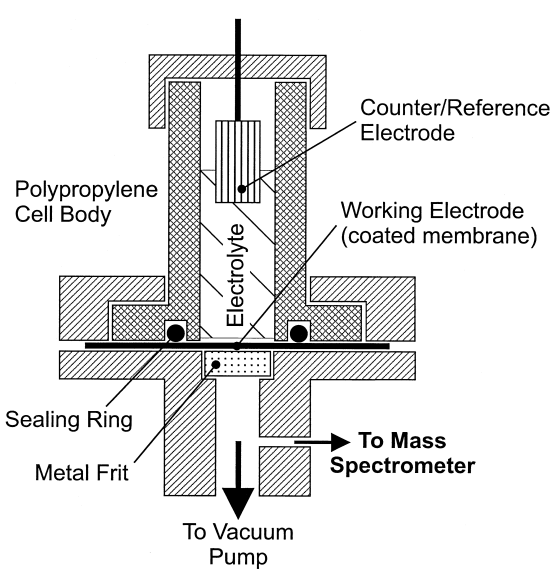

Fig. 3. The electrochemical cell for in situ DEMS.

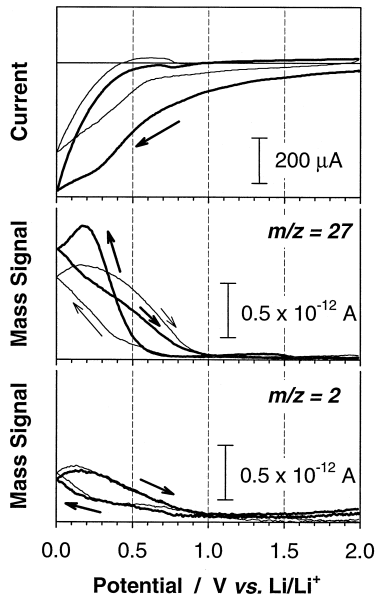

Fig. 4. CV (top) and two MSCVs (center and bottom) recorded in the electrolyte 1 M $LiPF_6$ in EC/DMC (1:1) at an ~75 μm thick graphite Timrex® SFG 6 electrode (bold line, first cycle; thin line, second cycle). The MSCVs exhibit mass signals $m/z = 27$ and $m/z = 2$, representing ethylene and hydrogen, respectively. The scan rate was 0.4 mV/s.

Using DEMS, we were able to show in a direct way that during the first charging of graphite electrodes different gases are evolved, an effect which can be correlated with current peaks in the CVs that are attributed to SEI formation [23,25]. Fig. 4 shows a typical DEMS experiment with a Timrex® SFG 6 electrode (about 75 μm thick, with a porosity of about 70%) in the battery electrolyte Merck LP30 [27]. The evolution of ethylene and hydrogen is typical for the EC/DMC electrolyte, but the difference between these results and those obtained earlier on much thinner electrodes (< 10 μm) is striking. In particular, it is clear from Fig. 4 that the SEI formation process, which is responsible for ethylene evolution [26], is not complete during the first cycle. Thus, an effective SEI film formation on practical thick electrodes requires much more time than expected on the basis of earlier experiments involving thin model electrodes. Moreover, using DEMS, we studied the oxidative decomposition of carbonate-based electrolyte solutions on lithium metal oxide composite electrodes [23] and were able to conclude that CO_2 is evolved in most cases. However, in EC-based electrolytes, much less CO_2 is evolved than with propylene

carbonate (PC). At $LiNiO_2$ composite electrodes in EC/DMC-based electrolytes, CO_2 was detected at potentials as low as 4.2 V vs. Li/Li^+. In contrast, both at $LiCoO_2$ and $LiMn_2O_4$ composite electrodes we saw no CO_2 formation up to a potential of 5.5 V vs. Li/Li^+. Thus, when compared with $LiNiO_2$, both $LiCoO_2$ and $LiMn_2O_4$ will provide a much higher safety margin with respect to the problem of gas evolution on overcharge.

4. In situ infrared spectroscopy

During both the electrochemical reduction and oxidation of electrolyte solutions in lithium-ion batteries, surface films containing organic and inorganic compounds are formed on the respective electrodes [28,29]. High-vacuum techniques normally applied for the analysis of surface films do not reflect the state of the film in situ [30]. Because of its molecular specificity, infrared (and/or Raman) spectroscopy would be an ideal method if it could be applied in situ. Two major problems have to be solved. First, the electrolyte solution strongly absorbs infrared light. Thus, thin-layer external reflectance or, alternatively, internal reflectance techniques must be used [30]. Second, there is a problem of sensitivity if very low absorptions from species on or near an electrode have to be detected. This problem can be overcome by subtracting spectra recorded at different potentials. Under optimum conditions, the sensitivity of infrared detection of, e.g., CO_2 is much higher then with the DEMS [31].

Our experimental approach is based on the subtractively normalized interfacial fourier transform infrared spectroscopy (SNIFTIRS) technique [30]. A hermetically sealed spectro-electrochemical cell designed for measurements in water and oxygen-free environment is used (Fig. 5). It is a thin layer, one-compartment cell provided with a plane optical window (CaF_2 or ZnSe). The cell is installed in the FTIR spectrometer with the surface of the working electrode in a horizontal position. Thus, relative to a conventional SNIFTIRS cell much less electrolyte is needed. The construction details are described in reference [32]. The working electrode is a mechanically polished glassy carbon disc spray-coated with a thick layer of, e.g., graphite with binder. Alternatively, for investigations of reactions occurring at current collectors the working electrode is made from polished copper, aluminum, or nickel metal. The potential-dependent changes at the electrode/electrolyte interface and/or in the thin electrolyte layer between the electrode and the optical window are visualized by plotting R_E/R_0, where R_E is the reflectance single beam spectrum taken at the working electrode potential and R_0 the background single beam spectrum taken usually at the open-circuit potential.

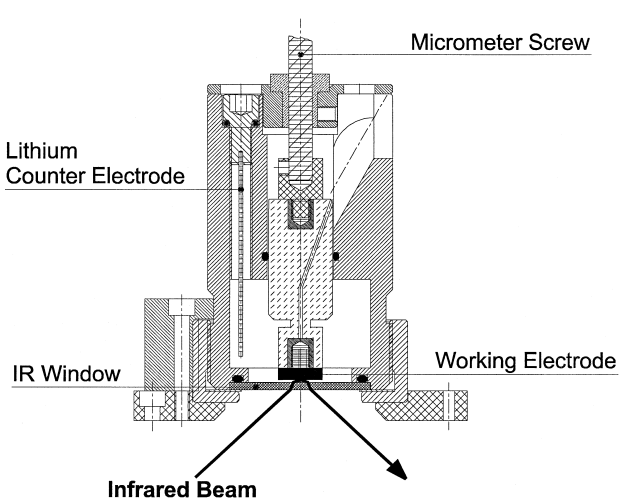

Fig. 5. The electrochemical cell for in situ infrared spectroscopy.

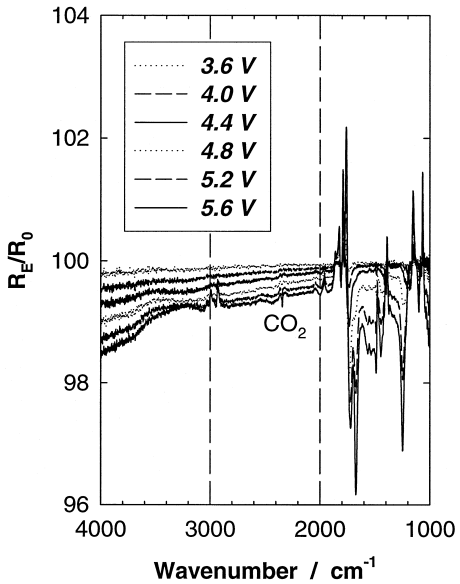

Fig. 6. SNIFTIR spectra measured on a polished nickel electrode in the electrolyte 1 M $LiPF_6$ in EC over a potential interval from 3.6 to 5.6 V vs. Li/Li^+.

The results shown in Fig. 6 have been selected to demonstrate what happens in lithium-ion cells during overcharge. Electrolyte solutions based on PC, EC, DMC, and their mixtures are readily oxidized at nickel current collectors at the working potentials of charged positive electrodes in lithium-ion batteries (≥ 4 V vs. Li/Li^+). However, the oxidation of EC-based electrolytes (Fig. 6) yields much less CO_2 than the oxidation of PC. No CO_2 evolution was observed during DMC oxidation. In an electrolyte mixture based on EC/DMC, the component with the higher dielectric constant, EC, is preferentially oxidized [33]. Thus, in future attempts to optimize the electrolytes of the EC/DMC type for commerical cells, major attention should be given to lowering the oxidation rate of the high-dielectric-constant component in the solvent mixture [32,33].

5. In situ Raman microscopy

In lithium-ion batteries, carbonaceous materials are used in both electrodes. One of the open questions is the change occurring under continuous cycling in the microstructure of the carbons. Raman spectroscopy is well suited for an analysis of the structural properties of carbonaceous materials [34–36]. Moreover, the electroactive oxides used in positive electrodes can readily be characterized also using Raman spectroscopy [37,38]. Unfortunately, the surfaces of the electrodes are not homogeneous; they typically reveal one or two types of carbon and/or an oxide, a binder, and occasionally an additive. Thus, a lateral resolution at the electrode surface corresponding to a typical particle size of a few micrometers must be achieved in order to be able to characterize each component in a working electrode individually. For this type of investigations, in situ Raman microscopy is a suitable technique.

In Fig. 7, we show the schematic drawing of the in situ Raman cell developed by us [39], where electrodes from commercial batteries can be used as test samples. We work with a confocal Raman microscope (LabRam, DILOR/Instruments) using the 530.901 nm line of an external Kr^+ ion laser. By using a microscope with an ultralong-working-distance objective (Olympus) with 50 × magnification it is possible to obtain good quality Raman spectra from a depth of up to ca. 0.3 mm below the sapphire optical window. With the pinhole diameter adjusted to 200 μm, the lateral resolution is 4 μm according to manufacturer specifications. The laser power was adjusted to 3–4 mW in order to avoid damage to the electrode surface.

Measurements performed by us on graphite-based electrodes during the first lithium intercalation/de-intercalation cycle confirmed the published results [12,36]. In addition, mapping techniques were applied to show that lithium intercalation does not proceed homogeneously all across a carbon electrode [26]. Here we demonstrate for the first time that the Raman technique is also suitable for an in situ characterization of single oxide particles in positive electrodes of lithium-ion cells. As an example, a Raman spectrum measured at a $LiCoO_2$ particle randomly selected on the surface of a commercial electrode is shown in Fig. 8.

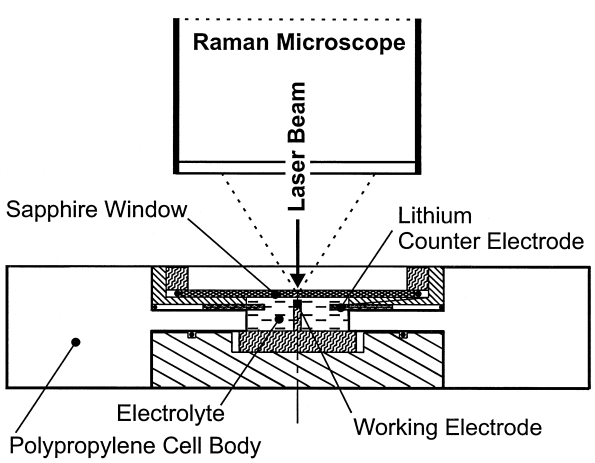

Fig. 7. The electrochemical cell for in situ Raman microscopy.

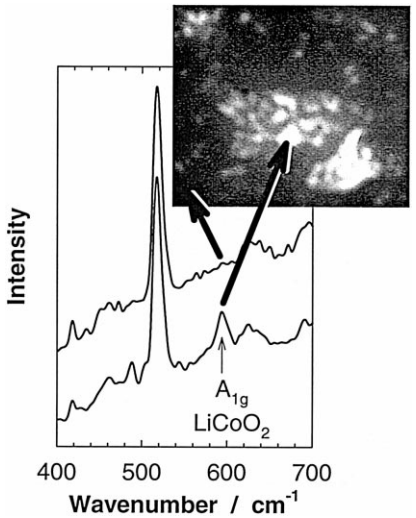

Fig. 8. In situ Raman spectra measured on open circuit at the surface of a commercial $LiCoO_2$ electrode in the electrolyte 1 M $LiClO_4$ in EC/DMC (1:1). In the photograph obtained with an optical microscope, which covers an area of ca. 15×15 μm, the arrows indicate the points where the two spectra were measured.

The spectra in Fig. 8 confirm that the light-colored particle in the photograph is $LiCoO_2$, whereas no spectral features of the oxide are observed in the dark region. Spectra of this $LiCoO_2$ particle recorded one after the other during the first galvanostatic charging are shown in Fig. 9. The band assigned to the A_{1g}-mode of $LiCoO_2$ is vanishing with increasing potential rapidly, in agreement with results reported in the literature [40]. This behavior

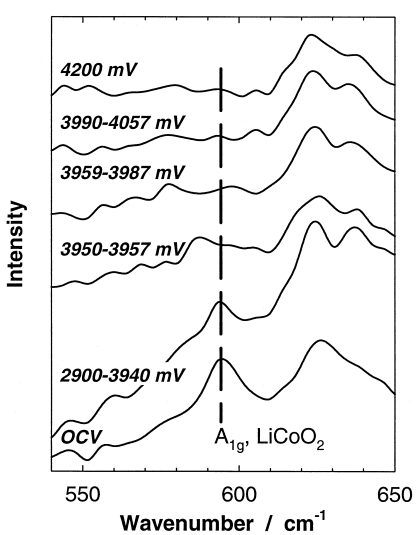

Fig. 9. Raman spectra recorded in situ during charging of a commercial $LiCoO_2$ electrode in the electrolyte 1 M $LiClO_4$ in EC/DMC (1:1). Potential in mV vs. Li/Li^+; the traces were shifted vertically.

was explained with an increase of the electrical conductivity by about two orders of magnitude in $Li_{1-x}CoO_2$, for $x > 0.04$ [41]. Interestingly, the E_{2g} band of $LiCoO_2$ is observed with only very low intensity in the in situ spectra (Fig. 10, bottom), although the magnitude of this band is about half of that of the A_{1g}-mode in a reference material [40]. A superimposition of Raman bands of EC, DMC, ClO_4^- and the features of $LiCoO_2$ does not explain the weakness of the E_{2g}-mode since Fig. 8 shows that bands of the electrolyte and $LiCoO_2$ are sufficiently separated. Thus, the orientation of the $LiCoO_2$ particle with respect to the polarization of the laser beam is supposed to be responsible.

A possible future application of the in situ Raman technique is to use it as a fingerprint technique to judge the quality of battery materials after repeated cycling. The feasibility of such an approach is demonstrated in Figs. 10 and 11. Fig. 10 shows two diagrams: the top one displays the time-dependence of the potential of the $LiCoO_2$ electrode and the off-band background intensity recorded in a spectral region where no Raman bands were observed. Both charging and discharging steps were followed by open circuit (OCV) periods of 1-h duration. Whereas the off-band intensity is roughly constant during the first charging half cycle (lithium de-insertion), it increases during the discharging half cycle (lithium insertion), and drops rapidly after the current is switched off. The letters A, B and C indicate the points where the corresponding Raman spectra displayed in the bottom part of Fig. 10 were recorded. The spectrum of the electrolyte solution was subtracted from these spectra after normalization, and the traces were shifted vertically. Trace A, recorded at the beginning of the experiment, shows clearly the A_{1g}-mode at 595 cm^{-1}, and a weak feature at a position where the E_{2g}-band would have been expected. After charging, the features due to $LiCoO_2$ are not observable (trace B). At potentials negative to 3700 mV, the band assigned to the A_{1g}-mode emerges again, as demonstrated with spectrum C recorded in the OCV period (calculated band position 594 cm^{-1}). The signal intensity of the A_{1g}-mode is lower than that originally observed (trace A), and its linewidth is slightly increased. This indicates that after the electrochemical cycle, the $LiCoO_2$ phase is slightly more lithium-deficient [40]. Fig. 11 compares the in situ spectrum recorded before cycling with a spectrum obtained after four deep galvanostatic cycles, recorded after 2 h at a constant potential of 2.75 V vs. Li/Li^+. The ratio of the intensity of the A_{1g}-band to the electrolyte band at 518 cm^{-1} helps to compare the spectra — it is lower for the cycled material by about 20%.

In summary, we show that Raman microscopy is feasible for in situ analyses of electrode materials. The results indicate subtle changes in these materials during cycling. As shown by us earlier on graphite electrodes [39], Raman microscopy is capable to monitor the lithium-ion concen-

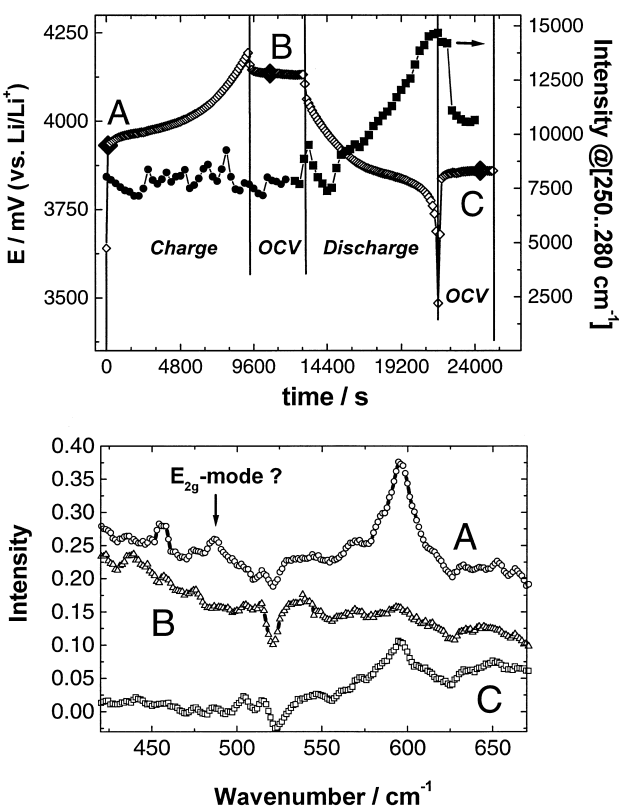

Fig. 10. (Top) Time dependence of the potential, E, of a commercial $LiCoO_2$ electrode during galvanostatic cycling in the electrolyte 1 M $LiClO_4$ in EC/DMC (1:1) and the off-band background Raman intensity recorded in a spectral region where no Raman bands were observed. (Bottom) Raman spectra of $LiCoO_2$ recorded in situ at the points A, B, and C. The spectrum of the electrolyte solution was subtracted after normalization, and the traces were shifted vertically.

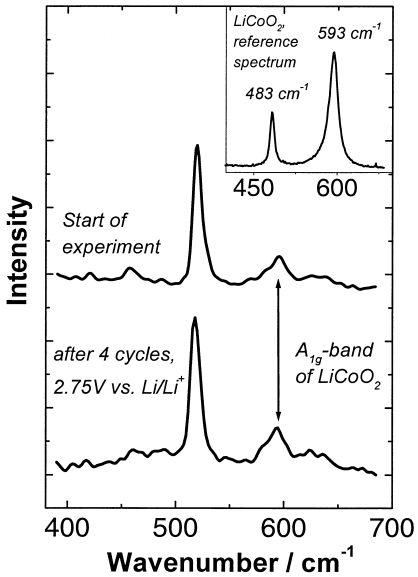

Fig. 11. Raman spectra recorded in situ during cycling of a commercial $LiCoO_2$ electrode in the electrolyte 1 M $LiClO_4$ in EC/DMC (1:1). Top: before cycling; bottom: after four deep galvanostatic cycles (the spectrum was recorded after equilibration for 2 h at a constant potential of 2.75 V vs. Li/Li^+.). The inset shows a reference spectrum of $LiCoO_2$ recorded ex situ.

tration at the electrode/electrolyte interface by analyzing the background intensity recorded at various potentials. Common to both positive and negative electrodes is that, upon lithium insertion into the host material, the background intensity rises significantly, whereas upon lithium de-insertion from the host material the background intensity is nearly constant. Thus, an optical method is available to study the ion transport at the interface.

6. Conclusions

It follows from our in situ experiments on electrodes of practical thickness that in some cases in lithium-ion batteries, the electrochemical processes do not proceed homogeneously at different sites of the electrode surface. Moreover, significant differences exist between the results obtained in model systems and those obtained at practical electrodes. We conclude that more care need to be exercised in applying some of the models suggested in the literature to the complex electrochemistry of lithium-ion batteries.

Acknowledgements

This work was supported in part by the Swiss Federal Office of Energy, Bern. We thank B. Rykart and Ch. Marmy for technical assistance and Dr. O. Haas, Paul Scherrer Institute, Prof. A. Wokaun, Paul Scherrer Institute, and Prof. R. Nesper, Swiss Federal Institute of Technology, Zurich for fruitful discussions.

References

[1] T. Ohzuku, Four-volt cathodes for lithium accumulators and the Li-ion batteries concept, in: G. Pistoia (Ed.), Lithium Batteries. New Materials, Developments and Perspectives, Elsevier, Amsterdam, 1994, p. 239.
[2] M. Jean, A. Chaussé, R. Messina, Electrochim. Acta 43 (1998) 1795.
[3] D. Aurbach, B. Markovsky, M.D. Levi, E. Levi, A. Schechter, M. Moshkovich, Y. Cohen, J. Power Sources 81–82 (1999) 95.
[4] D. Bar-Tow, E. Peled, L. Burstein, J. Electrochem. Soc. 146 (1999) 824.
[5] G.H. Wrodnigg, J.O. Besenhard, M. Winter, J. Electrochem. Soc. 146 (1999) 470.
[6] R.R. Chianelli, J.C. Scanlon, B.M.L. Rao, J. Electrochem. Soc. 125 (1978) 1563.
[7] J.R. Dahn, M.A. Py, R.R. Haering, Can. J. Phys. 60 (1982) 307.
[8] G. Eggert, J. Heitbaum, Electrochim. Acta 31 (1986) 1443.
[9] P. Novák, P.A. Christensen, T. Iwasita, W. Vielstich, J. Electroanal. Chem. 263 (1989) 37.
[10] P. Krtil, L. Kavan, K. Macounová, J. Electroanal. Chem. 433 (1997) 187.
[11] K. Kanamura, J. Power Sources 81–82 (1999) 123.
[12] M. Inaba, H. Yoshida, Z. Ogumi, T. Abe, Y. Mizutani, M. Asano, J. Electrochem. Soc. 142 (1995) 20.
[13] D.E. Irish, Z. Deng, M. Odziemkowski, J. Power Sources 54 (1995) 28.
[14] M. Inaba, Z. Siroma, A. Funabiki, Z. Ogumi, T. Abe, Y. Mizutani, M. Asano, Langmuir 12 (1996) 1535.
[15] F. Kong, J. Kim, X. Song, M. Inaba, K. Kinoshita, F. McLarnon, Electrochem. Solid State Lett. 1 (1998) 39.
[16] M. Winter, J.O. Besenhard, M.E. Spahr, P. Novák, Adv. Mater. 10 (1998) 725.
[17] Z. Ogumi, M. Inaba, Bull. Chem. Soc. Jpn. 71 (1998) 521.
[18] B.A. Johnson, R.A. White, J. Power Sources 70 (1998) 48.
[19] D. Billaud, E. McRae, A. Hérold, Mater. Res. Bull. 14 (1979) 857.
[20] X.Y. Song, K. Kinoshita, T.D. Tran, J. Electrochem. Soc. L120 (1996) 143.
[21] F. Joho, B. Rykart, R. Imhof, P. Novák, M.E. Spahr, A. Monnier, J. Power Sources 81–82 (1999) 243.
[22] H. Yoshida, T. Fukunaga, T. Hazama, M. Terasaki, M. Mizutani, M. Yamachi, J. Power Sources 68 (1997) 311.
[23] R. Imhof, P. Novák, J. Electrochem. Soc. 146 (1999) 1702.
[24] R. Imhof, P. Novák, in: C.F. Holmes, A.R. Landgrebe (Eds.), Proceedings of the Symposium on Batteries for Portable Applications and Electric Vehicles, Electrochem. Soc. Proc. Ser. vol. 97-18 1997, p. 313.
[25] R. Imhof, P. Novák, J. Electrochem. Soc. 145 (1998) 1081.
[26] P. Novák, F. Joho, R. Imhof, J.-C. Panitz, O. Haas, J. Power Sources 81–82 (1999) 212.
[27] M. Lanz, P. Novák, Electrochim. Acta (2000) submitted.
[28] D. Aurbach, B. Markovsky, I. Weissman, E. Levi, Y. Ein-Eli, Electrochim. Acta 45 (1999) 67.
[29] T. Eriksson, T. Gustafsson, J.O. Thomas, in: S. Surampudi, R. Marsh (Eds.), Lithium Batteries, Electrochem. Soc. Proc. Ser. vol. 98-16 1998, p. 315.
[30] P.A. Christensen, A. Hamnett, in: R.G. Compton, A. Hamnett (Eds.), Chemical Kinetics: New Techniques for the Study of Electrodes and Their Reactions vol. 29 Elsevier, Amsterdam, 1989, p. 1.
[31] M. Winter, R. Imhof, F. Joho, P. Novák, J. Power Sources 81–82 (1999) 818.
[32] F. Joho, PhD Thesis No. 11745, ETH Zurich, Switzerland (1996).
[33] F. Joho, P. Novák, Electrochim. Acta (2000) in press.
[34] F. Tuinstra, J.L. Koenig, J. Chem. Phys. 53 (1970) 1126.
[35] L. Nikiel, P.W. Jagodzinski, Carbon 31 (1993) 1313.
[36] W. Huang, R. Frech, J. Electrochem. Soc. 145 (1998) 765.
[37] X. Zhang, R. Frech, J. Electrochem. Soc. 145 (1998) 847.
[38] W. Huang, R. Frech, J. Power Sources 81–82 (1999) 616.
[39] J.-C. Panitz, F. Joho, P. Novák, Appl. Spectrosc. 53 (2000) 1188.
[40] M. Inaba, Y. Iriyama, Z. Ogumi, Y. Todzuka, A. Tasaka, J. Raman Spectrosc. 28 (1997) 613.
[41] M. Ménétrier, I. Saadoune, S. Levasseur, C. Delmas, J. Mater. Chem. 9 (1999) 1135.